Laboratory Investigation

Stereotactic and Functional Neurosurgery

Stereotact Funct Neurosurg 2004;82:156–164
DOI: 10.1159/000081639

Published online: October 19, 2004

MRI Changes in the Rat Hippocampus following Proton Radiosurgery

James D. Rabinov[a] Jonathan L. Brisman[c] Andrew J. Cole[e]
Patricia Lani Lee[b] Marc R. Bussiere[d] Paul H. Chapman[c] Jay S. Loeffler[d]
G. Rees Cosgrove[c] Tina Chaves[a] R. Gilberto Gonzalez[a, b]

[a]Division of Neuroradiology, Department of Radiology, [b]MGH-NMR Center, [c]Department of Neurosurgery, [d]Department of Radiation Oncology/Harvard Cyclotron, [e]Department of Neurology, Massachusetts General Hospital and Harvard Medical School, Boston, Mass., USA

Key Words
Radiation injury · Animal model · Proton radiosurgery · MRI

Abstract
Purpose: To define radiographic dose-response relationships for proton radiosurgery using a rat brain model. ***Methods and Materials:*** A group of 23 rats was treated with Bragg peak proton beam irradiation involving the right hippocampus. Single doses of 5, 12, 20, 30, 60, 90 and 130 cobalt gray equivalents (CGE) were delivered to groups of 3 animals using single fraction technique. One extra animal was included at the 130- and 30-CGE doses. Animals were imaged using a standard 1.5-tesla GE Signa MRI. A 3-inch surface coil was employed to obtain T_1-weighted sagittal images (TR 600 and TE 30) and dual echo T_2-weighted coronal images (TR 3,000 and TE 30/90). Animals were imaged at 1.5, 3, 4.5, 6 and 9 months. Volumetric analysis with custom software was done to evaluate areas of increased signal on T_2-weighted images, and signal change versus time curves were generated. Gadolinium-enhanced T_1-weighted imaging was also done at the 9-month time point to further evaluate tissue injury. The development of hydrocephalus was also examined. ***Results:*** Peak tissue injury was greater and occurred earlier with higher versus lower doses of radiation. Statistically significant differences were seen between the 130- and 90-CGE animals and between the 90- and 60-CGE animals ($p < 0.0016$) using ANOVA. Signal changes can be seen in at least 1 of the animals at 20 CGE. The largest volume of tissue enhancement at 9 months was seen in animals at 60 CGE, which may represent an intermediate zone of tissue injury and gliosis compared with greater tissue loss at higher doses and less injury at lower doses. Hydrocephalus developed first in the untreated hemisphere in 130- and 90-CGE animals as a result of mass effect while it occurred at a later time in the treated hemisphere in lower-dose animals. ***Conclusions:*** Following single-dose proton radiosurgery of rat hippocampus, serial MRIs show T_2 signal changes in animals ranging from 130 down to 20 CGE as well as the development of hydrocephalus. Dose-effect relationships using proton radiosurgery in rats will be a helpful step in guiding further studies on radiation injury to brain tissue.

KARGER
Fax + 41 61 306 12 34
E-Mail karger@karger.ch
www.karger.com

1011–6125/04/0824–0156$21.00/0

Accessible online at:
www.karger.com/sfn

James D. Rabinov, MD
Department of Neuroradiology/Clinics 363
Massachusetts General Hospital, 55 Fruit Street
Boston, MA 02114 (USA)
Tel. +1 617 726 1767, Fax +1 617 724 3338, E-Mail jrabinov@partners.org

Introduction

Radiosurgery is in widespread use in the treatment for brain tumors and arteriovenous malformations with doses of 14–17 cobalt gray equivalents (CGE) [1]. It is currently in trials for ablative therapy of functional disorders such as intractable epilepsy [2, 3] with temporal lobe doses of 21–50 Gy and for Parkinson's disease [4] in which thalamic doses of 100–165 Gy have been utilized. It is important to define changes in brain tissue from these therapeutic doses as a process separate from tumor or other disease processes in affected patients. Our goal is to define the extent and time course of signal changes on T_2-weighted and gadolinium-enhanced MRI in a rat brain model of proton radiosurgery to the hippocampus.

Methods and Materials

Twenty-three male Sprague-Dawley descendent rats (25–350 g; Charles River Laboratories, Wilmington, Mass., USA) were irradiated using Bragg peak stereotactic radiosurgery to the right hippocampus. Proton beam delivery was accomplished with the design of a stereotactic head frame that could be mounted in a clinical beam line at the Harvard Cyclotron Laboratory. The head frame was constructed of lucite and incorporated a bite block and internal immobilizing bars. It was determined that a single dorsal portal would provide the sharpest dose gradient between the right and left hippocampi [5, 6]. The beam line selected for this rodent experiment is routinely used for the treatment of ocular lesions in humans because of its sharp lateral penumbra (80–20% dose gradient over 1.6 mm) and distal falloff (80–20% dose gradient over 5.0 mm) [7]. As described in a previous publication [8], we used rat atlas coordinates to design a brass aperture conform to the lateral and longitudinal projections of the center of the right hippocampus. The aperture dimension included a 2.5-mm margin except along the midline edge where no margin was added. This margin is required to allow for a 1.5-mm 90–50% penumbra with a 1.0-mm edge definition and alignment uncertainty. The 90 and 50% values represent the dose prescription level and the dose at the aperture edge, respectively. Groups of 3 animals were irradiated at doses of 5, 12, 20, 30, 60, 90 and 130 CGE. The conversion factor to comparable photon radiation is CGE $\times 1.1$ = Gy.

A computed tomography (CT) scan was obtained of a representative rat using the stereotactic head frame. The CT scan allowed the rat atlas dimensions to be confirmed, and provided conversion factors to precisely predict the depth to which the proton beam penetrates the tissue. It is at this point of deepest penetration that most of the beam's energy is transferred to the target. This is the so-called Bragg peak. Tissues beyond this point receive no radiation dose. Proton beam penetration is defined as a water equivalent depth. Mapping the hippocampus on the atlas and applying the effective depth conversion factors defined the proximal (2.3 mm) and distal (5.6 mm) extents to be covered by the prescribed dose. The measured nonmodulated proton beam with the custom brass aperture had proximal and distal prescription depths of 0.8 and 5.5 mm from the skull, respectively.

The alignment technique used for this experiment relied on projecting a light through the beam-defining aperture onto the exposed rodent skull. The sagittal and coronal suture and bregma are well defined and provide good alignment references. The medial and anterior aperture edges were placed 0.5 mm from the sagittal suture and anterior to the bregma, respectively. Differential doses were administered depending on the treatment protocol. Reproducible immobilization, operative exposure and irradiation of each animal took approximately 10 min with a set-up accuracy better than 0.5 mm.

The 23 animals were imaged at the intervals of 1.5, 3, 4.5, 6 and 9 months following irradiation. Animals were sedated with intraperitoneal pentobarbital (50 mg/kg) and imaged using a 1.5-tesla GE Signa MRI scanner. A 3-inch surface coil was employed to obtain 3-mm T_1-weighted images (TR 600 ms and TE 30 ms) and dual-echo T_2-weighted coronal images (TR 3,000 ms and TE 30/90 ms). T_1-weighted axial images were also obtained if an abnormality was detected on the T_2-weighted images. Off-line analysis was performed with a semi-automated perimeter-based technique to evaluate areas of increased signal on the T_2-weighted images. Point-to-point analysis was used to identify areas of 25% signal increase compared with contralateral gray and white matter. This threshold was employed to minimize the chance of false-positive interpretation. For each animal an index slice was identified on the T_2-weighted images estimated to match the isodose center selected according to the rat atlas. In some cases, hydrocephalus developed. When it was bilateral, the ventricles were excluded from the volume of parenchymal change since it was likely due to communicating or obstructive hydrocephalus. When the right lateral ventricle was larger, only a volume comparable to the untreated left side was excluded. This region was considered to represent tissue loss following treatment. A volume of tissue with T_2 abnormality was generated from the coronal images of the animals at each time point and plotted individually and also by dosage group.

After 9 months, a gadolinium-enhanced T_1-weighted sequence was obtained in all animals. Venous access was accomplished with a femoral vein cutdown on anesthetized animals. A 1-mm French silastic catheter was placed in the right femoral vein and sewn in place for the experiment. A saline flush syringe was attached and flushed every 3 min. Gadolinium (Magnevist) was administered at a dose of 0.2 cm^3/kg which is similar to a double dose of contrast in humans. Volume of enhancement was evaluated in a similar manner as T_2 signal change.

Volumetric curves were generated for each animal and also for each dosage group. Statistical analysis was performed using ANOVA methodology with 1 variable within and 1 in between. Intra-observer statistical analysis was also carried out using a linear regression model after independent evaluation of 10 random individual time points.

All experiments were conducted in accordance with the guidelines for animal care set forth by the Subcommittee for Research and Animal Care of Massachusetts General Hospital. Rats were housed on a 24-hour light/dark cycle and given free access to food and water. Metallic ear tags were used to track animal identity.

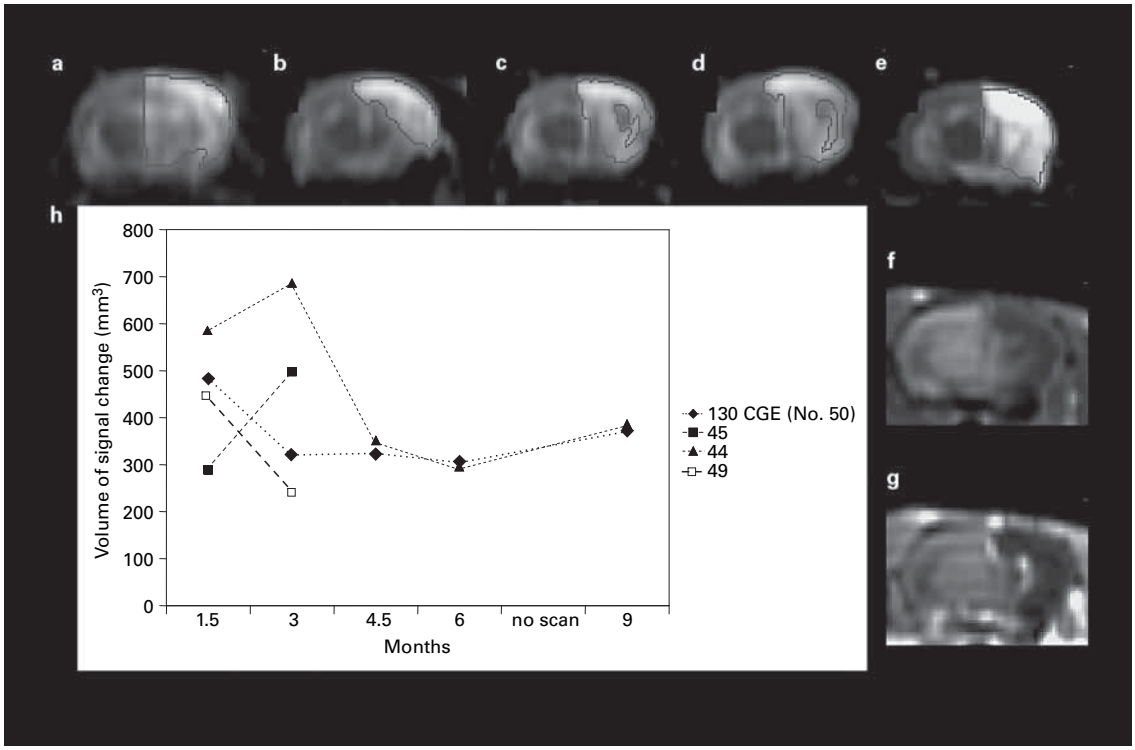

Fig. 1. Coronal T_2-weighted index slices (the isodose center) from animal No. 50 in the 130-CGE dose group (**a–e**). Pre- (**f**) and post-gadolinium (**g**) coronal images showing cystic encephalomalacia with rim enhancement at 9 months. **h** Signal change versus time curves for the animals in the 130-CGE group. Time points of 1.5, 3, 4.5, 6 and 9 months are included with outlines at the 25% signal change compared with contralateral tissue. Maximum changes were seen at or before 3 months in all animals.

Results

Four animals were sacrificed at the 3-month interval for histopathologic evaluation [7]; all other animals survived to the 9-month time point. In general, signal changes on MRI were centered on the index slice, the focus of treatment according to treatment planning from the rat atlas. Figures 1a–e show the T_2-weighted coronal images from animal No. 50 taken from the index slice. Figure 1h shows the volume of T_2 signal change versus time curves from the 130-CGE rats. These 130-CGE rats were either at peak or early resolution phase of radiation injury at the first imaging time point of 6 weeks. Figures 2a–e show sequential time points with the volumetric outlines taken from the index slices of animal No. 46 from the 90-CGE dose group. The T_2 volume versus time plots for the 90-CGE animals show peak volume changes at the 3- to 4.5-month range as shown in figure 2h. The 60-CGE animals show signal changes which are less severe and delayed compared with the 90-CGE animals. Figures 3a–e show the index slices from animal No. 40, a 60-CGE animal with the volumetric outlines of T_2 signal change. The plots of these animals are shown in figure 3h demonstrating peak T_2 volume changes at 6 months or

Fig. 2. Coronal T_2-weighted index slices from animal No. 46 in the 90-CGE dose group (**a–e**). Pre- (**f**) and post-gadolinium (**g**) coronal images showing cystic encephalomalacia with rim enhancement at 9 months. **h** Signal change versus time curves for the animals in the 90-CGE group. Time points of 1.5, 3, 4.5, 6 and 9 months are included with outlines at the 25% signal change compared with contralateral tissue. Maximum changes were seen at or between 3 and 4.5 months.

Fig. 3. Coronal T_2-weighted index slices from animal No. 40 in the 60-CGE dose group (**a–e**). Pre- (**f**) and post-gadolinium (**g**) coronal images showing cystic encephalomalacia with rim enhancement at 9 months. **h** Signal change versus time curves for the animals in the 60-CGE group. Time points of 1.5, 3, 4.5, 6 and 9 months are included with outlines at the 25% signal change compared with contralateral tissue. Maximum changes were seen at 6 months or later.

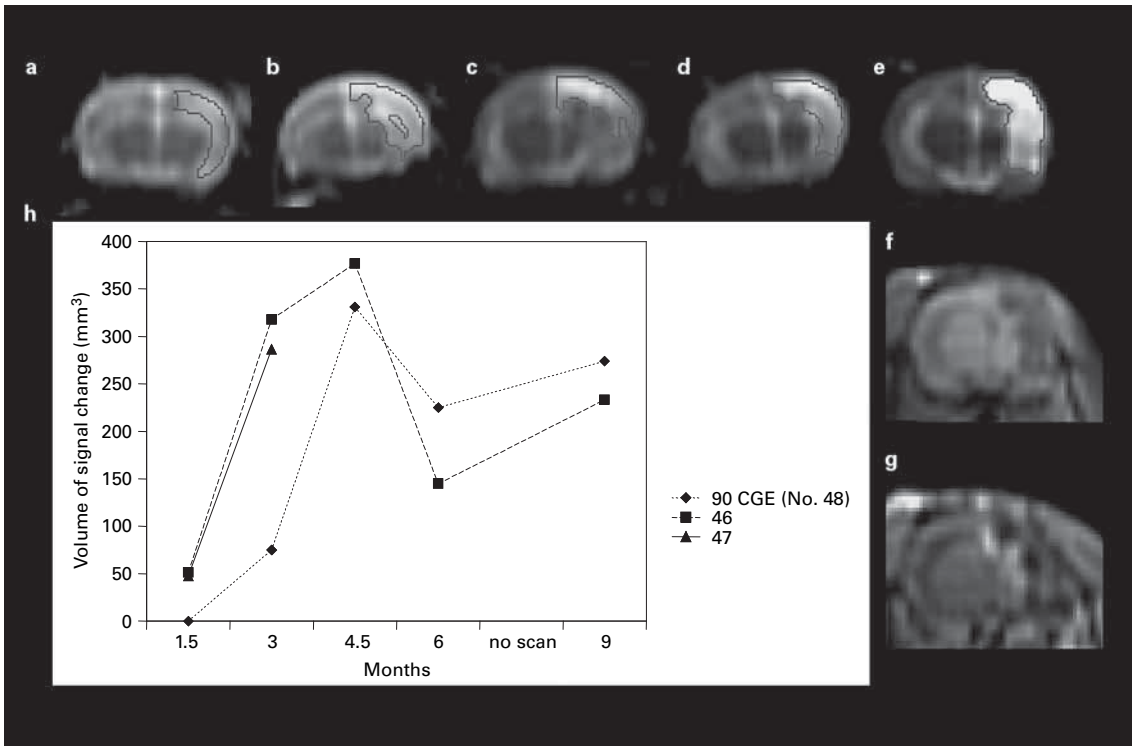

2

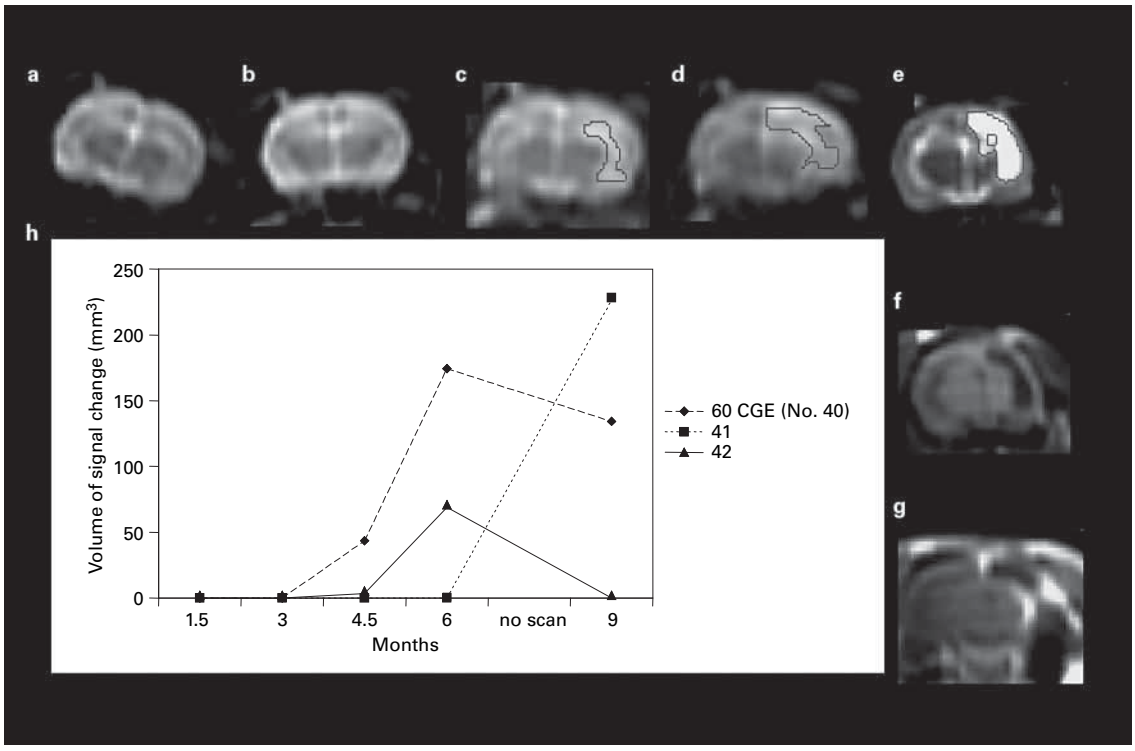

3

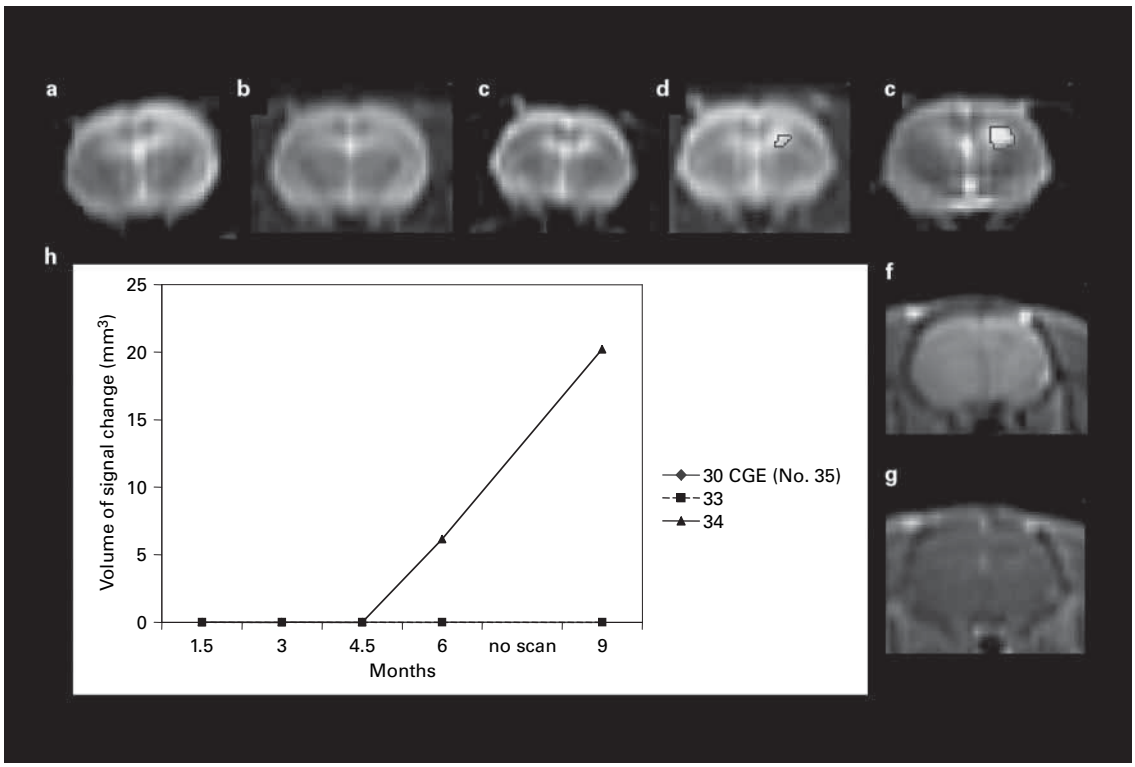

Fig. 4. Coronal T_2-weighted index slices from animal No. 34 in the 30-CGE dose group (**a–e**). Pre- (**f**) and post-gadolinium (**g**) coronal images showing a small focus of enhancement at 9 months at the site of irradiation. **h** Signal change versus time curves for the animals in the 30-CGE group. Time points of 1.5, 3, 4.5, 6 and 9 months are included with outlines at the 25% signal change compared with contralateral tissue. Signal changes are seen at 6 months.

more. The 30-CGE animals are beginning to show changes by the 6-month time point in figure 4h and the 20-CGE animals may show changes as early as 4.5 months in figure 5h. When the data are plotted with averages from each group, it is evident that at lower doses, there is less tissue damage. Also, for diminishing dose of radiation, the T_2 signal changes are delayed in onset.

Statistically significant changes are seen between the volume of T_2 signal change comparing the 60- and the 90-CGE animals and also between the 90- and the 130-CGE animals ($p < 0.0016$) using ANOVA (fig. 6).

Post-gadolinium coronal images average volumes of enhancing tissue in the 130-CGE animals was 29.29 mm^3, in the 90-CGE animals 55.08 mm^3, in the 60-CGE animals 92.29 mm^3 and in the 30-CGE animals 22.07 mm^3. There was cystic encephalomalacia with partial rim enhancement in animals at doses from 60 to 130 CGE. There was no evidence for hyperintensity on T_1-weighted images prior to gadolinium, so methemoglobin was not present in a significant amount to cause signal change.

Animals at doses ranging from 30 to 130 CGE developed ventricular enlargement. When it was asymmetric or unilateral on the affected side, it was considered the result of tissue loss. Hydrocephalus was seen in all of the 130-CGE animals beginning at 3 months. Figure 7a–e shows developing hydrocephalus in rat No. 44, a 130-CGE animal, through the 1.5-, 3-, 4.5-, 6- and 9-month time points. The pattern began with dilatation of the left lateral ventricle related to mass effect from swelling, followed by moderate bilateral hydrocephalus as the acute changes subsided. The 90-CGE rats all showed hydrocephalus which began at the 4.5-month time point as shown in animal No. 48 (fig. 7f–j). Two of 3 animals at 60 CGE developed mild hydrocephalus right greater than left, and 1 of the 30-CGE animals developed minimal dilatation on the right.

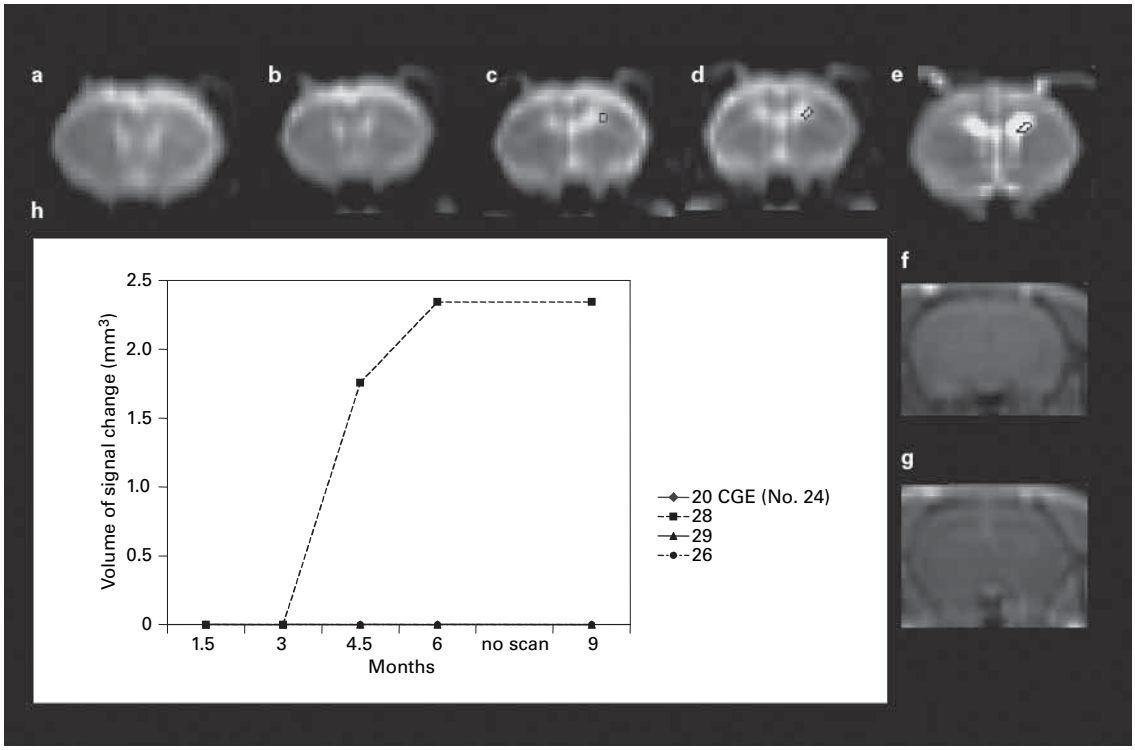

Fig. 5. Coronal T_2-weighted index slices from animal No. 28 in the 20-CGE dose group (**a–e**). Pre- (**f**) and post-gadolinium (**g**) coronal images showing no definite enhancement at 9 months. **h** Signal change versus time curves for the animals in the 20-CGE group. Time points of 1.5, 3, 4.5, 6 and 9 months are included with outlines at the 25% signal change compared with contralateral tissue. T_2 signal changes may be seen as early as 4.5 months.

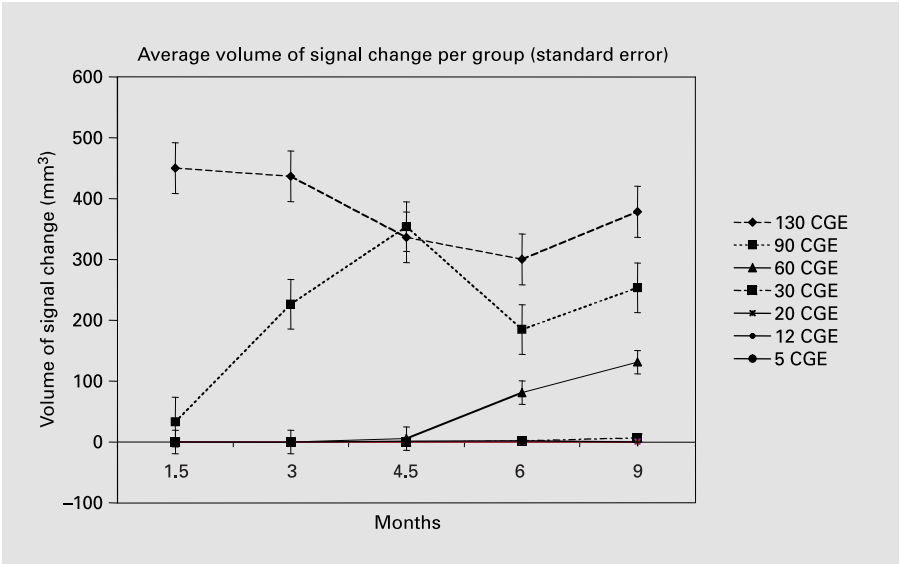

Fig. 6. Signal change versus time curves at different doses. At higher doses, signal abnormalities were detected earlier and with larger volumes of affected tissue.

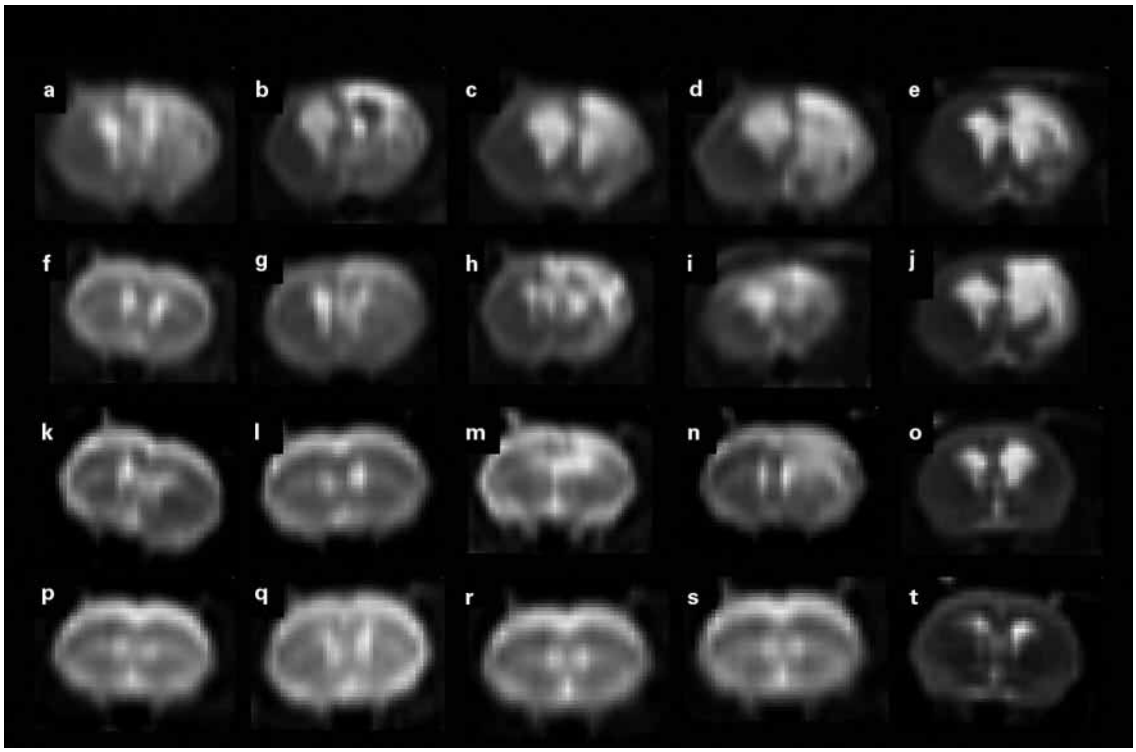

Fig. 7. a–e Development of hydrocephalus in animal No. 44 from the 130-CGE dose group. Time points at 1.5, 3, 4.5, 6 and 9 months show that hydrocephalus develops first on the untreated side by 3 months as a result of entrapment. Follow-up images show that the right lateral ventricle eventually enlarges as the acute radiation changes evolve into encephalomalacia. **f–j** This pattern is also seen in the 90-CGE animals, taken from animal No. 48. However, there is a delay of approximately 1.5 months. **k–o** At the 60-CGE level, unilateral hydrocephalus develops right greater than left at 9 months as in animal No. 40. **p–t** Minimal ventricular dilation on the right at 9 months in animal No. 35, a 30-CGE animal.

Discussion

This study describes the dose-related MRI changes seen in the rat hippocampus after Bragg peak proton radiosurgery. The targeted tissue could be localized with a highly conformal dose distribution. The volumetric analysis of T_2 signal changes over the course of 9 months shows that for higher doses of radiation, there is a larger region of tissue damage. The time until the peak of greatest reaction within brain tissue is delayed as the dose of radiation decreases. In spite of the small number of animals included in the study, there is a statistically significant difference between the 60- and 90-CGE and also between the 90- and 130-CGE groups.

Several research groups have published data which are consistent with specific aspects of our findings; the most extensive studies by Kondziolka et al. [9] date from 1992. Their group treated rats with photon radiosurgery with varying doses from 30–200 Gy and followed them for 90 days. They saw no pathologic changes at doses of 60 Gy or below. Necrosis could be seen at doses of 100 Gy and higher. Mild reactive changes were seen at 70- and 80-Gy levels. Since we followed our animals further in time, delayed changes in the lower-dose animals became apparent. Calvo et al. [10] identified demyelination and white matter necrosis in rats at doses of 22.5 Gy at 26 weeks following radiotherapy. Kennedy et al. [11] also showed that there is a time delay for changes in animals at lower doses compared with higher doses. They found that animals at the 50-Gy level began to show changes such as ventricular dilatation at 14.6 weeks following treatment, 35-CGE animals began to show changes at 35 weeks and animals as low as 25 Gy began to show changes at 40.4 weeks. Liscak et al. [12] found changes at 50 Gy, but not at 25 Gy. Animals from our own lab sacrificed at 3 months showed necrosis at the 130-CGE level. At 90 CGE, there were areas of necrosis, edema, inflammation, neuronal loss and vascular dilatation. At the 30- and 60-

CGE levels, gliosis and endothelial cell thickening were seen at the 3-month time point [8].

Gadolinium enhancement reflects disruption of the blood brain barrier. Gadolinium was administered at the 9-month time point. The postcontrast images at the higher doses of 60–130 CGE indicate a rim of enhancing tissue with cystic encephalomalacia. These data represent the later phase of necrosis, that of glial scar surrounding a region of tissue loss. In the 60-CGE animals, there is the largest volume of enhancing tissue, likely representing an intermediate phase of tissue injury, repair and early glial scar with a rim of vascular proliferation. Qualitatively, the volume of cystic change was greater for high-dose animals. In all 3 of the 30-CGE animals, there is a small focus of enhancement in the right hippocampus representing a more subtle degree of radiation injury, possibly with an inflammatory response or simply endothelial injury. A T_2 signal can be seen in some of these animals. From the data, it is difficult to predict whether T_2-weighted imaging or gadolinium enhancement is more sensitive to radiation changes, but the variability likely reflects the different phases of radiation injury and repair among individuals. Prior studies have looked at this phenomenon resulting from injury to blood vessel endothelium. Omary et al. [13] noted gadolinium enhancement at 4 weeks following a 120-Gy dose to rat brain tissue, but did not have T_2-weighted imaging for comparison. Richards and Budinger [14] noted that Evans blue dye could be found in the brain surrounding brain tissue treated with doses of 50 Gy as early as 4 days, but more clearly at 3 months at both 30 Gy and 50 Gy. Karger et al. [6] showed that there is a larger time delay to the onset of enhancement with lower doses. At 9 months only, the 100-Gy animals showed enhancement, while at 18 months, animals with doses as low as 30 Gy showed some enhancement. Remler et al. [15] treated rats with single doses of 20–60 Gy. They found that at doses of 60 Gy, 83% of the animals had leakage of Evans blue dye (examined at 98 days), whereas 58% of the animals receiving 20 Gy showed leakage of the dye (examined at 217 days). Since the time of imaging differs significantly, it is unclear from these data whether animals are in different stages along the curve of injury and repair or whether they exhibit different degrees of injury altogether.

Hydrocephalus developed along 1 of 2 courses. For the 130- and 90-CGE animals, hydrocephalus appeared in the left hemisphere first. It was always seen earlier in the higher-dose animals. This is likely due to obstructive physiology resulting from swelling in the treated right hemisphere. Subsequently, ventricular dilatation occurred on the right. This may be the result of tissue loss, obstruction from scarring, cellular debris or a communicating hydrocephalus. We included only the asymmetric portion of it as tissue loss or T_2 signal change. Our group suggests that this method minimized any misinterpretation about the etiology of the change while allowing for some ex vacuo enlargement of the ipsilateral ventricle. For animals at the 60- and 30-CGE levels, hydrocephalus developed on the treated side first. Again, only the asymmetric volume was considered for T_2 signal change from tissue loss.

Radiation injury includes a spectrum of changes affecting blood vessels, glial cells and neurons [16–24]. In patients undergoing radiotherapy, changes within the first 2 weeks are the result of a radiation-induced vasculopathy. These acute changes are infrequently seen at fractionated doses of 60 Gy. The changes are manifested by brain edema, increased intracranial pressure and seizure. Early delayed changes, seen in up to 30% of patients, occur 6–8 weeks following treatment. Late changes of radiation necrosis typically occur 6–36 months following treatment. They can result in a progressive and sometimes lethal inflammatory reaction. Subacute changes are not predictive of this delayed process. Several differences between humans and these rodents exist. The life span of these animals is significantly smaller than in humans.

Therefore, the changes we observed are likely to be compressed in time. The second point is that these animals have a significantly smaller proportion of white matter than humans. It is known that white matter is more sensitive to radiation than gray matter.

Our study was designed to determine the time course for the development and maturation of discrete hippocampal lesions by MRI appearance using T_2-weighted and gadolinium-enhanced imaging techniques. There is a range of therapeutic radiation used in patients which includes 14–17 CGE for AVMs up to 100- to165-Gy thalamic doses for the treatment of Parkinson's disease. It is important to develop animal models in which to assess normal brain response to radiation injury. By separating radiation changes from primary disease processes, one can begin to design and follow treatment algorithms in these models.

Acknowledgements

The authors would like to express their appreciation to the following people who aided in conducting this research: Drs. A. F. Thornton and T. Hedley-Whyte were helpful in an advisory capacity during the initial stages of the project. J. Ren and M. Bradley-Moore were helpful in animal work for the imaging component of the study.

References

1 Chapman PH: Personal communication with review of 2 years of data from Massachusetts General Hospital, July 20, 2004.

2 Grabenbauer GG, Reinhold CH, Kerling F, et al: Fractionated stereotactically guided radiotherapy of pharmacoresistant temporal lobe epilepsy. Acta Neurochir Suppl 2002;84:65–70.

3 Hajek M, Dezortova M, Liscak R, et al: ^{1}H MR spectroscopy of mesial temporal lobe epilepsies treated with gamma knife. Eur Radiol 2003;13:994–1000.

4 Duma CM, Jacques DB, Kopyov OV, et al: Gamma knife radiosurgery for thalamotomy in parkinsonian tremor: A five-year experience. J Neurosurg 1998;88:1044–1049.

5 Kamiryo T, Berr SS, Berk HW, et al: Accuracy of an experimental stereotactic system for MRI-based gamma knife irradiation in the rat. Acta Neurochir (Wien) 1996;138:1103–1107.

6 Karger CP, Hartman GH, Hoffmann U, et al: A system for stereotactic irradiation and magnetic resonance evaluations in the rat brain. Int J Radiat Oncol Biol Phys 1995;33:485–492.

7 Gragoudas ES, Seddon J, Goitein M, et al: Current results of proton beam irradiation of uveal melanomas. Ophthalmology 1985;92:284–291.

8 Brisman JL, Cole AJ, Cosgrove GR, et al: Radiosurgery of the rat hippocampus: Magnetic resonance imaging, neurophysiological, histological and behavioral studies. Neurosurgery 2003;53:951–961.

9 Kondziolka D, Lunsford LD, Claassen D, et al: Radiobiology of radiosurgery. 1. The normal rat brain model. Neurosurgery 1992;31:271–279.

10 Calvo W, Hopewell JW, Reinhold HS, et al: Time- and dose-related changes in the white matter of the rat brain after single doses of X rays. Br J Radiol 1988;61:1043–1052.

11 Kennedy AS, Archambeau JO, Archambeau MH, et al: Magnetic resonance imaging as a monitor of changes in the irradiated rat brain. An aid in determining the time course of events in a histologic study. Invest Radiol 1995;30:214–220.

12 Liscak R, Vladyka V, Novotny J Jr, et al: Leksell gamma knife lesioning of the rat hippocampus: Relationship between radiation dose and functional and structural damage. J Neurosurg 2002;97(suppl 5):666–673.

13 Omary RA, Berr SS, Kamiryo T, et al: Gamma knife irradiation-induced changes in the normal rat brain studied with ^{1}H magnetic resonance spectroscopy and imaging. Acad Radiol 1995;2:1043–1051.

14 Richards T, Budinger TF: NMR imaging and spectroscopy of the mammalian central nervous system after heavy ion radiation. Radiat Res 1988;113:79–101.

15 Remler MP, Marcussen WH, Tiller-Borsich J: The late effects of radiation on the blood brain barrier. Int J Radiat Oncol Biol Phys 1986;12:1965–1969.

16 Andersson B, Larsson B, Leskell L, et al: Histopathology of late local radiolesions in the goat brain. Acta Radiol Ther Phys Biol 1970;9:385–394.

17 Blatt DR, Friedman WA, Bova FJ, et al: Temporal characteristics of radiosurgical lesions in an animal model. J Neurosurg 1994;80:1046–1055.

18 Hassler O: Microangiopathic studies on changes in the cereral vessels after irradiation. 2. Proton beam lesions in the rat. Acta Radiol Ther Phys Biol 1966;4:394–400.

19 Kamiryo T, Kassell NF, Thai QA, et al: Histologic changes in the normal rat brain after gamma irradiation. Acta Neurochir (Wien) 1996;138:451–459.

20 Larsson B, Leksell L, Rexed B, et al: The high-energy proton beam as a neurosurgical tool. Nature 1958;182:1222–1223.

21 Lo EH, Frankel KA, Steinberg GK, et al: High-dose single-fraction brain irradiation: MRI, cerebral blood flow electrophysiological and histological studies. Int J Radiat Oncol Biol Phys 1992;22:47–55.

22 Mori Y, Kondziolka D, Balzer J, et al: Effects of stereotactic radiosurgery on an animal model of hippocampal epilepsy. Neurosurgery 2000;46:157–165.

23 Rexed B, Mair W, Sourander P, et al: Effect of high-energy protons on the brain of the rabbit. Acta Radiologica 1960;53:289–299.

24 Rogers M, Myers R, Jenkinson T, et al: Histology of the irradiated rat brain in the first post-irradiation year. Br J Radiol 1982;55:208–212.